J Biomol NMR (2010) 48:137–145
DOI 10.1007/s10858-010-9444-6

ARTICLE

High-resolution methyl edited GFT NMR experiments for protein resonance assignments and structure determination

Garima Jaipuria · Anushikha Thakur · Patrick D'Silva · Hanudatta S. Atreya

Received: 19 May 2010 / Accepted: 9 August 2010 / Published online: 14 September 2010

Abstract Three-dimensional (3D) structure determination of proteins is benefitted by long-range distance constraints comprising the methyl groups, which constitute the hydrophobic core of proteins. However, in methyl groups (of Ala, Ile, Leu, Met, Thr and Val) there is a significant overlap of ^{13}C and ^{1}H chemical shifts. Such overlap can be resolved using the recently proposed (3,2)D HCCH-COSY, a G-matrix Fourier transform (GFT) NMR based experiment, which facilitates editing of methyl groups into distinct spectral regions by combining their ^{13}C chemical shifts with that of the neighboring, directly attached, ^{13}C nucleus. Using this principle, we present three GFT experiments: (a) (4,3)D NOESY-HCCH, (b) (4,3)D ^{1}H-TOCSY-HCCH and (c) (4,3)D ^{13}C-TOCSY-HCCH. These experiments provide unique 4D spectral information rapidly with high sensitivity and resolution for side-chain resonance assignments and NOE analysis of methyl groups. This is exemplified by (4,3)D NOESY-HCCH data acquired for 17.9 kDa non-deuterated cytosolic human J-protein co-chaperone, which provided crucial long-range distance constraints for its 3D structure determination.

Keywords NOESY · TOCSY · GFT NMR · Methyl-edited NOESY · Protein structure

Electronic supplementary material The online version of this article (doi:10.1007/s10858-010-9444-6) contains supplementary material, which is available to authorized users.

G. Jaipuria · A. Thakur · H. S. Atreya (✉)
NMR Research Centre, Indian Institute of Science, Bangalore 560012, India
e-mail: hsatreya@sif.iisc.ernet.in

G. Jaipuria · A. Thakur
Solid State and Structural Chemistry Unit, Indian Institute of Science, Bangalore 560012, India

A. Thakur
Chemical Biology Programme, Indian Institute of Science, Bangalore 560012, India

A. Thakur · P. D'Silva (✉)
Department of Biochemistry, Indian Institute of Science, Bangalore 560012, India
e-mail: patrick@biochem.iisc.ernet.in

Introduction

High-resolution structure determination of proteins by NMR spectroscopy relies on a large network of ^{1}H–^{1}H NOEs, which provide long range distance information or constraints between ^{1}H nuclei (Wüthrich 1986). Important among these are constraints involving methyl-methyl and methyl-non-methyl protons (Gardner et al. 1997; Zheng et al. 2003). This is primarily due to the fact that methyl groups constitute the hydrophobic core of globular proteins and come close in three-dimensional (3D) space to other methyl groups or hydrophobic groups, which are buried in the core of proteins. Further, their fast rotation coupled with three chemically equivalent protons renders them very sensitive thus making them favorable probes for structure determination (Tugarinov and Kay 2005). In recent years, a number of methods have been developed to exploit these characteristics for structural and dynamic studies in large molecular weight proteins (Gardner et al. 1996, 1997; Gross et al. 2003; Rosen et al. 1996; Tugarinov et al. 2003, 2004, 2005a, b; Tugarinov and Kay 2004a, Zwahlen et al. 1998).

In methyl groups (of Ala, Ile, Leu, Met, Thr and Val) there is a significant overlap of ^{13}C and ^{1}H chemical shifts (Atreya and Chary 2001). Typically, their ^{13}C and ^{1}H shifts fall in the range of 5–25 ppm and 0–1.5 ppm, respectively

(Fig. 1; statistical analysis based on chemical shift data of non-homologous 186 proteins taken from the BioMagResBank (BMRB; http://www.bmrb.wisc.edu)). This overlap is aggravated in multidimensional NMR experiments (specifically a 3D experiment), where one of the 2D projections happens to contain ^{13}C–^{1}H correlations. A 4D ^{13}C–^{13}C NOESY (Kay et al. 1991; Clore et al. 1991) or its variants (Anglister et al. 1994; Grzesiek et al. 1995; Lee et al. 1994; Muhandiram et al. 1993a, b; Vuister et al. 1993) can help resolve such overlap. However, their acquisition with high resolution for structural analysis is hampered by long minimal measurement times. While rapid data collection methods for these experiments have been proposed (Coggins et al. 2005; Farmer and Mueller 1994; Galius et al. 2008; Kock and Griesinger 1994; Shen et al. 2005; Snyder et al. 2007a, b; Tugarinov et al. 2005a, b; Xia et al. 2003, 2008), the overlap of ^{13}C and ^{1}H chemical shifts of methyl groups (Fig. 1a) has not been addressed. This is also applicable to ^{13}C-edited TOCSY experiments routinely used for protein resonance assignments (Cavanagh et al. 2007; Kay et al. 1993; Logan et al. 1992).

We have recently developed an experiment (Barnwal et al. 2008) based on G-matrix Fourier transform NMR spectroscopy (Atreya and Szyperski 2005; Kim and Szyperski 2003; Szyperski and Atreya 2006), which overcomes this limitation and facilitates rapid acquisition of spectra with high resolution. The experiment, namely, methyl edited GFT (3,2)D HCCH-COSY exploits the fact that while the ^{13}C chemical shifts of the different methyl groups overlap, their directly one-bond attached neighboring carbon nuclei have distinct ^{13}C chemical shifts for the different amino acid types (Barnwal et al. 2008). For instance, $^{13}C^{\alpha}$ of alanine, which is directly attached to its methyl carbon ($^{13}C^{\beta}$) has a distinct chemical shift (50–55 ppm) than $^{13}C^{\beta}$ of threonine ($\sim$70 ppm) which is directly attached to its methyl carbon ($^{13}C^{\gamma 2}$; Cavanagh et al. 2007). Thus, by combining the chemical shift of a methyl carbon with its directly attached neighboring carbon nucleus, a distinct separation of methyl groups is obtained (illustrated in Fig. 1). The utility of (3,2)D HCCH-COSY was demonstrated for stereo specific assignment of methyl groups of leucine and valine (Barnwal et al. 2008). This methodology can be incorporated in a ^{13}C-edited NOESY or TOCSY experiment in the resolving dimension such that methyl groups get edited in one of the 2D projections of a 3D experiment. This forms the basis of HCCH edited GFT (4,3)D ^{1}H-^{1}H NOESY, ^{1}H and ^{13}C TOCSY experiments proposed here. These experiments provide 4D spectral information rapidly with high sensitivity and resolution for resonance assignment and structure determination. The proposed method has been used for obtaining long range distance constraints in a non-deuterated 17.9 kDa cytosolic human J-protein co-chaperone (rotational correlation time (τ_c) of $\sim$10 ns) a highly conserved protein, which plays

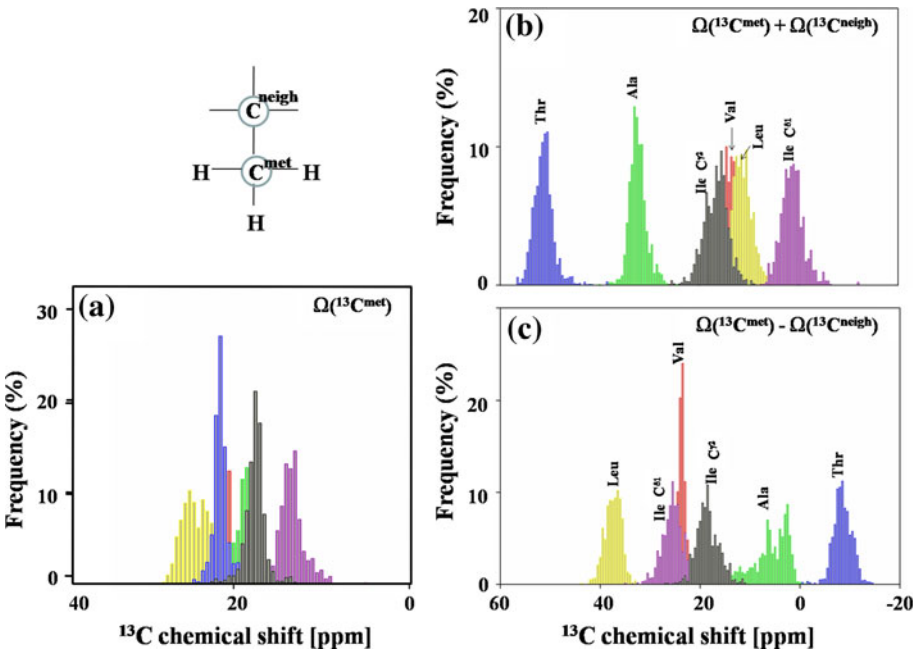

Fig. 1 Histogram plots showing distribution of chemical shifts of **a** methyl carbons (indicated as $\Omega(^{13}C^{met})$), **b** $\Omega(^{13}C^{met}) + \Omega(^{13}C^{neigh})$ and **c** $\Omega(^{13}C^{met}) - \Omega(^{13}C^{neigh})$. The linear combinations are defined as: $\Omega(^{13}C^{met}) \pm *\Omega(^{13}C^{neigh}) = \delta^{met} \pm (\delta^{neigh} - \delta^{carrier\ \ frequency})$ (where δ is the chemical shift value). A ^{13}C carrier frequency of 40 ppm was chosen for calculation. The schematic drawing of the molecular structure (*top*) defines $^{13}C^{met}$ and $^{13}C^{neigh}$. The statistical analysis for obtaining these chemical shift distributions was carried out using database of non-homologous 186 proteins taken from the BioMagResBank (BMRB)

crucial role in protein folding (Qiu et al. 2006). These experiments are applicable to uniformly ^{13}C-labeled protein samples with partial deuteration or samples prepared using the SAIL approach (Kainosho et al. 2006).

Materials and methods

NMR spectroscopy

Figure 2 depicts schematically the magnetization transfer pathway and Fig. 3 shows the radio-frequency (RF) pulse schemes of the three experiments proposed: (a) (4,3)D NOESY-HCCH, (b) (4,3)D ^{1}H-TOCSY-HCCH and (c) (4,3)D ^{13}C-TOCSY-HCCH. For the nuclei shown underlined, the chemical shift evolution periods are jointly co-incremented. The (4,3)D NOESY-HCCH provides ^{1}H–^{1}H shift correlations as in a conventional NOESY, whereas (4,3)D ^{1}H-TOCSY-HCCH and (4,3)D ^{13}C-TOCSY-HCCH spectra provide intra-residue ^{1}H and ^{13}C shift correlations, respectively. A detailed product operator treatment of the experiments is provided in the supplementary material and briefly discussed below. The complete set of pulse sequences, parameters, processing scripts and representative raw data sets are available from the authors upon request.

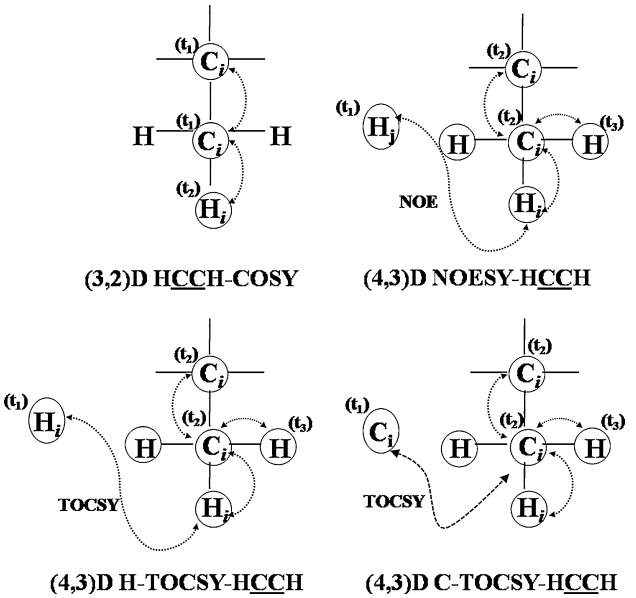

Fig. 2 A schematic drawing illustrating the magnetization transfer pathways implemented in the proposed (4,3)D GFT NMR experiments. The (3,2)D HCCH-COSY has been published previously (Barnwal et al. 2008). The letter '*i*' or '*j*' denotes the residue number along the polypeptide chain. Also indicated are the chemical shift evolution periods ('t_i'; $i = 1,2,3$) used for frequency labeling of different ^{13}C/^{1}H nuclei

Sample preparation

Ubiquitin containing plasmid (PGLUB) was transformed into *E. coli* BL21 cells. Cells were grown at 37°C in M9 minimal medium consisting of 1 g/L of $^{15}NH_4Cl$ and 4 g/L of ^{13}C-Glucose. Protein expression was induced at midlog phase ($OD_{600} \sim 0.6$) by addition of 1.0 mM isopropyl β-D-thiogalactoside (IPTG). Cells were harvested by centrifugation and solubilized in acetate buffer (5 mM EDTA, 50 mM Na acetate, pH 5). Following sonication, the supernatant containing the protein was loaded onto a pre-equilibrated ion exchange column (SP Sepharose fast flow from GE) and the protein eluted with a salt gradient of 0–0.6 M NaCl. For NMR studies, a sample containing $\sim$1.0 mM of protein in 50 mM Phosphate buffer (100% $^{2}H_2O$; pH 6.0) was prepared.

The open reading frame corresponding to cytosolic human J-protein was PCR-amplified from human HeLa cells cDNA library using sequence specific primers and cloned into a pET3a vector with a 6-Histidine tag at the C-terminus of the protein resulting in 155 amino acid residues (17.9 kDa). The constructs were transformed into *E. coli* Rosetta cells. The cells were grown at 30°C in M9 minimal medium consisting of 1 g/L of $^{15}NH_4Cl$ and 4 g/L of ^{13}C-Glucose and induced with 0.5 mM IPTG. The protein was purified using Ni–NTA column followed by gel filtration. The final NMR sample contained $\sim$0.7 mM protein, 20 mM Tris buffer (pH 7.5) and 80 mM NaCl in 100% $^{2}H_2O$.

NMR data collection

NMR experiments were performed at 25°C on a Bruker 700 MHz spectrometer equipped with a cryogenic probe (acquisition parameters and measurement times for the different experiments are provided in Table S1 of Supplementary Material). The ^{13}C r.f. carrier frequency was set to 40 ppm with a spectral width of 80 ppm to allow aliasing of peaks belonging to Threonine. The scaling factor, κ, was set to 1.0. Data were processed with NMRPipe (Delaglio et al. 1995) and analyzed using XEASY (Bartels et al. 1995). Since the G-matrix transformation is applied within the pulse sequence (Swain and Atreya 2008), the raw-data does not require any pre-processing and can be processed using methods used for conventional 3D FT-NMR spectra.

Results and discussion

Data acquisition

The magnetization transfer pathway implemented in the RF pulse schemes (Fig. 2) is briefly described as follows.

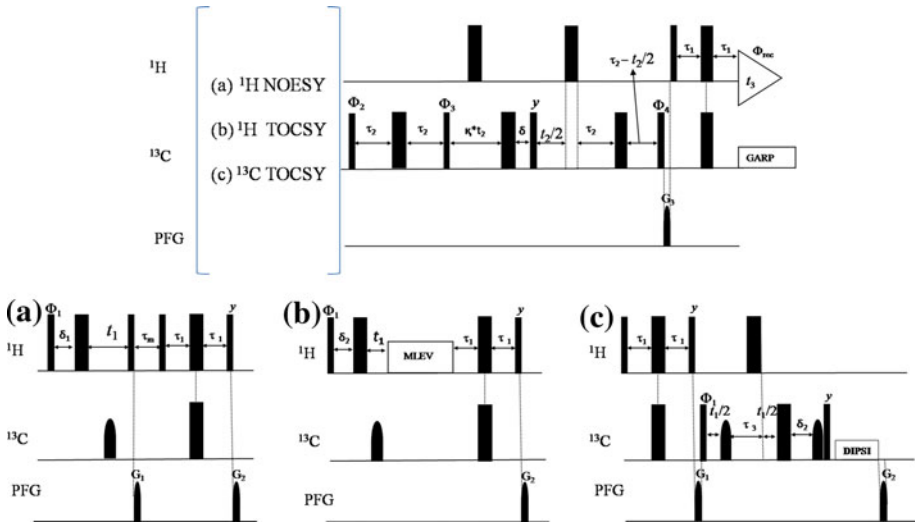

Fig. 3 R.f. pulse schemes of methyl edited GFT experiments: **a** (4,3)D NOESY-HCCH, **b** (4,3)D ^{1}H-TOCSY-HCCH and **c** (4,3)D ^{13}C-TOCSY-HCCH. All the three experiments share a common block which is indicated on the *top*. Rectangular 90° and 180° pulses are indicated by *thin* and *thick vertical bars*, respectively, and phases are indicated above the pulses. Where no r.f. phase is marked, the pulse is applied along *x*. High-power 90° pulse lengths are: 8.7 μs for ^{1}H, 37 μs for ^{15}N and 15.8 μs for ^{13}C. $\kappa = 1.0$ (see text). The ^{1}H r.f. carrier is placed at the position of the solvent line at 4.7 ppm. The ^{15}N carrier position is set to 118.5 ppm. The ^{13}C r.f. carrier is kept at 40 ppm throughout the sequence. GARP is employed to decouple ^{13}C during acquisition. All pulsed z-field gradients (PFGs) are sinc-shaped with gradient recovery delay of 200 μs. The duration and strengths of the PFGs are: G1-G3 (0.5 ms, 22 G/cm). The delays are: $\tau_1 = 1.7$ ms, $\tau_2 = 7.0$ ms, $\tau_3 = 1.1$ ms and $\delta = 30$ μs; δ_1, $\delta_2 = 500$ μs. Phase cycling: $\phi_1 = x$; $\phi_2 = x, y$; $\phi_3 = y, x$; $\phi_4 = x, y$; $\phi_{rec} = x, -x$ for all the three experiments. Quadrature detection along ω_1(^{1}H/^{13}C) is obtained by shifting the phase ϕ_1 by 90° in STATES or STATES-TPPI manner. Along ω_2 (^{13}C), the combination of phases: ϕ_2-ϕ_4 and ϕ_{rec} result in the selective detection of the linear combination: $\Omega(^{13}C_i^{met}) - \Omega(^{13}C_i^{neigh})$ (Swain and Atreya 2008). Alternatively, the second linear combination: $\Omega(^{13}C_i^{met}) + \Omega(^{13}C_i^{neigh})$ can be selectively detected by using the phase cycle: $\phi_2 = x, -y$; $\phi_3 = y, -x$; $\phi_4 = y, -x$; $\phi_{rec} = x, -x$

Following ^{1}H/^{13}C chemical shift evolution (during t_1) and a ^{1}H–^{1}H or ^{13}C–^{13}C mixing period, the magnetization resulting on a ^{13}C (methyl) nucleus (abbreviated as $^{13}C^{met}$) is transferred by one-bond J-coupling to its neighboring ^{13}C nucleus (abbreviated as $^{13}C^{neigh}$). The $^{13}C^{neigh}$ nucleus is frequency labeled during the chemical shift evolution period t_2. During the reverse transfer period, $^{13}C^{met}$ spins are frequency labeled in a constant-time manner. The delay, $2\tau_2$, is adjusted to $1/2J_{CC}$ ($\sim$14.0 ms; Fig. 3). Phase-sensitive joint-sampling of chemical shifts of $^{13}C^{met}$ and $^{13}C^{neigh}$ is achieved by co-incrementing their respective chemical-shift evolution periods with the $^{13}C^{neigh}$ shifts scaled by a factor 'κ' relative to $^{13}C^{met}$ (Atreya and Szyperski 2005; Szyperski and Atreya 2006). This results, after G-matrix transformation, in two sub-spectra each comprised of peaks at a given linear combination of chemical shifts along the indirect dimension (t_2): ω_2: $\Omega(^{13}C^{met}) \pm \kappa^*\Omega(^{13}C^{neigh})$, where the two ^{13}C nuclei belong to the same given amino acid and $\Omega(^{13}C^{met}) \pm \kappa^*\Omega(^{13}C^{neigh}) = \delta^{met} \pm \kappa^*(\delta^{neigh} - \delta^{carrier\ frequency})$ (δ is the chemical shift value). The scaling factor, κ, allows one to either increase the dispersion of peaks or restrict the chemical shift evolution period of ^{13}C to avoid loss in sensitivity due to transverse relaxation during t_2. In the present study, the scaling factor was set to 1.0. Thus, the following chemical shifts are detected in the different dimensions: ω_1: $^{1}H_{i/j}$/$^{13}C_{i/j}$; ω_2: $\Omega(^{13}C_i^{met}) \pm \Omega(^{13}C_i^{neigh})$; ω_3:$^{1}H_i^{met}$ where '*i/j*' refers to the residue number along the polypeptide chain. An additional 2D [^{13}C, ^{1}H] CT-HSQC recorded with the same sample provides central peak information (ω_1: $\Omega(^{13}C^{met})$) needed to analyze the data.

Further, as evident from Fig. 1, both linear combinations: $\Omega(^{13}C^{met}) \pm \Omega(^{13}C^{neigh})$ afford separation of chemical shifts of methyl groups into distinct spectral regions. Thus, either of the shift combination can be chosen and selectively detected using the method of combination shift selective GFT NMR approach (Swain and Atreya 2008). In this approach, the G-matrix transformation required for forming the desired linear combination is performed within the pulse sequence by appropriate phase cycling of the radiofrequency pulses and receiver avoiding thereby the need for any pre-processing of the data (Swain and Atreya 2008). In the present study, we acquired data with the linear combination: $\Omega(^{13}C^{met}) - \Omega(^{13}C^{neigh})$ which has a slightly better resolution (Fig. 1). This saves a measurement time by a factor 2 by avoiding the collection of the second undesired linear combination. Notably, an equivalent 4D NMR experiment with conventional sampling scheme and equivalent resolution would have required 30–40 fold higher measurement time due to sampling of an additional dimension.

(4,3)D NOESY-HCCH

Figure 4 shows the 2D {ω_2 (^{13}C), ω_3 (^{1}H)} projection of (4,3)D NOESY-HCCH spectrum of human J-protein in comparison with the corresponding projection of a 3D ^{13}C-edited [^{1}H, ^{1}H] NOESY-HSQC spectrum. The latter was recorded using the same acquisition parameters as used for (4,3)D GFT experiment (Table S1 of Supplementary material). Evidently, the 2D projection from the GFT experiment has higher dispersion and peaks belonging to the different methyl groups are well separated. Figure 5a shows representative {ω_1 (^{1}H), ω_3 (^{1}H)} plots from the (4,3)D NOESY-HCCH spectrum acquired for Ubiquitin in measurement time of $\sim$15.5 h. Figure 5b illustrates a few of the long-range NOEs mapped onto the 3D structure of the protein.

GFT data for the non-deuterated 17.9 kDa cytosolic human J-protein (0.7 mM; $\tau_c \sim 10$ ns) was acquired with a total measurement time of 43 h resulting in average S/N of $\sim 6 \pm 2$ for the long-range NOEs. Figure 6 shows representative {ω_1 (^{1}H), ω_3 (^{1}H)} strips from the (4,3)D NOESY-HCCH spectrum and Fig. 7 illustrates an example where methyl groups of V123 and T138 having similar $^{13}C^{met}$ chemical shifts of $\sim$21.5 ppm overlap in the conventional 3D ^{13}C-edited NOESY. They are resolved in the (4,3)D GFT spectrum (see also Fig. 4) due to differences in their $^{13}C^{neigh}$ chemical shifts ($^{13}C^{\beta}$ (V123) $\sim$35 ppm; $^{13}C^{\beta}$ (T138) $\sim$70 ppm), thereby facilitating accurate assignment of the NOEs. Note that the Threonine peaks are aliased to reduce the spectral width (Fig. 3). A total of 45 long range constraints involving methyl protons were obtained from GFT experiment which together with a 3D ^{15}N-edited NOESY provided crucial long range constraint for a high resolution 3D structure (to be published elsewhere). In order to validate the sensitivity of the method, a conventional 3D ^{13}C-resolved NOESY was acquired with the same acquisition parameters (i.e., spectral resolution) and measurement time (Table S1 of Supplementary material). All the expected long range ^{1}H–^{1}H correlations were observed in the (4,3)D GFT spectrum as compared to a conventional 3D spectrum.

(4,3)D ^{1}H-TOCSY-HCCH

The (4,3)D ^{1}H-TOCSY-HCCH complements the (4,3)D NOESY-HCCH experiment described above in that it provides the intra-residue ^{1}H correlations. In this experiment, ^{1}H magnetization is transferred to the methyl proton

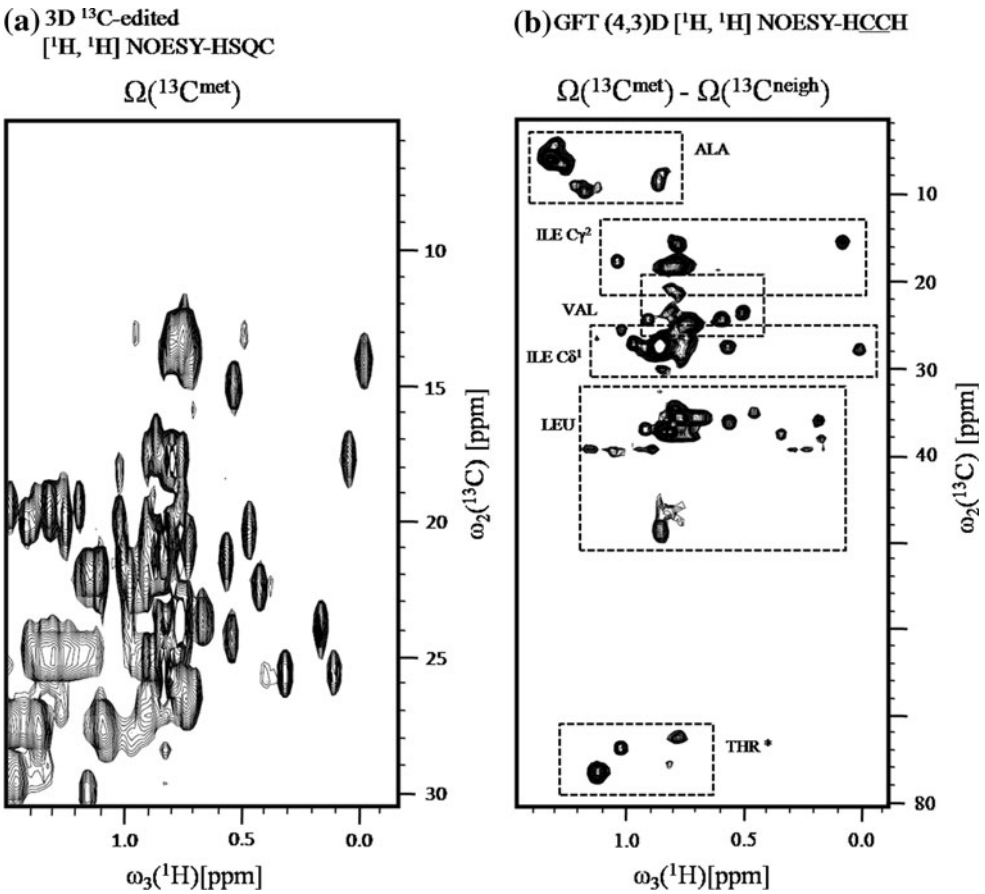

Fig. 4 Two-dimensional (2D) {ω_2 (^{13}C), ω_3 (^{1}H)} projections from **a** 3D ^{13}C-edited [^{1}H, ^{1}H] NOESY-HSQC of human J-protein in comparison with **b** the corresponding projection of a GFT (4,3)D NOESY-HCCH spectrum acquired and processed with similar spectral and digital resolution. Methyl groups in the GFT spectra belonging to different amino acids are indicated in by *boxed lines*. Peaks corresponding to Threonine are aliased to reduce the spectral width

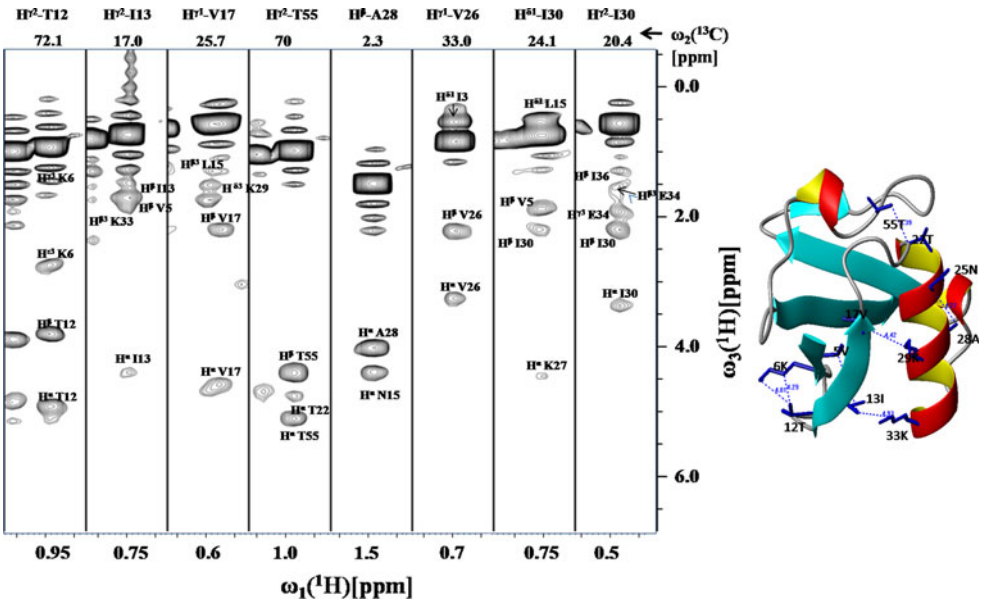

Fig. 5 **a** Representative $\{\omega_1$ (^{1}H), ω_3 (^{1}H)$\}$ strips from GFT (4,3)D NOESY-HCCH spectrum acquired for Ubiquitin and illustration of a few of the observed long-range NOEs mapped onto the 3D structure of ubiquitin (PDB code: 1UBQ). Chemical shifts along ω_2 ($\Omega(^{13}C^{met}) - \Omega(^{13}C^{neigh})$) and the residue number are indicated on the *top* of each strip. Labels on cross peaks in each strip indicate the respective chemical shift assignments. Peaks corresponding to Threonine are aliased (see Fig. 4)

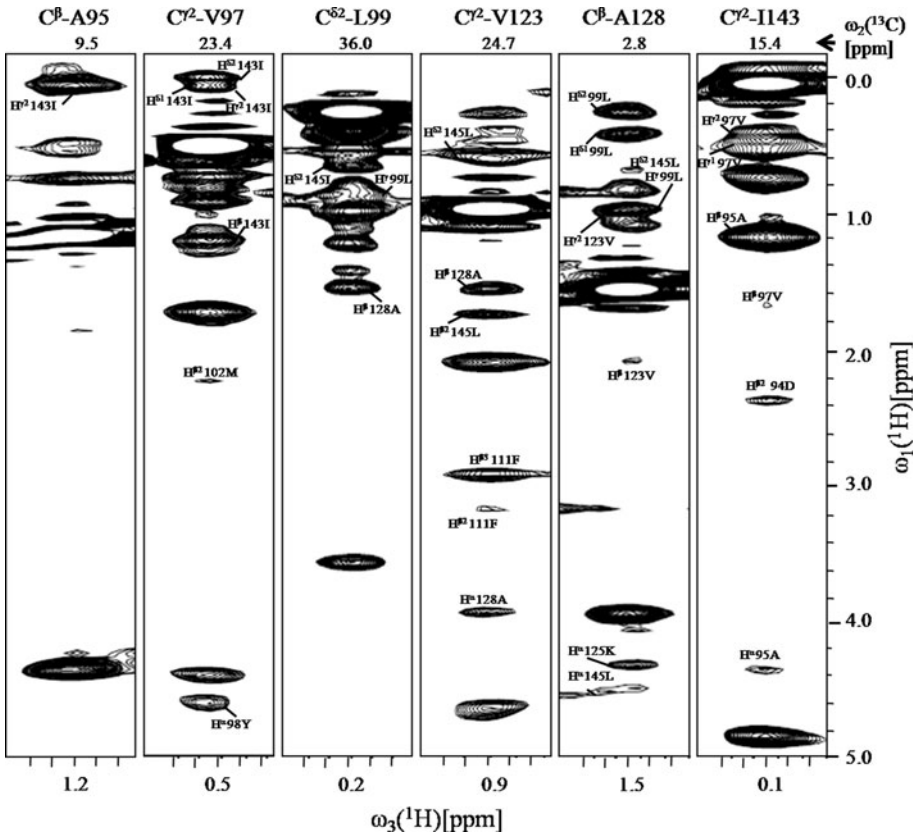

Fig. 6 Representative $\{\omega_1$ (^{1}H), ω_3(^{1}H)$\}$ strips from GFT (4,3)D NOESY-HCCH spectrum acquired for the 19 kDa human J-protein. Resonance assignment of cross peaks corresponding only to *long-range* NOEs is shown in each strip. The chemical shifts along ω_2 ($\Omega(^{13}C^{met}) - \Omega(^{13}C^{neigh})$) are indicated on the top. Peaks corresponding to Threonine are aliased (see Fig. 4)

within the same amino acid by isotropic mixing (Figs. 2 and 3). This is useful for assignments of peaks in the (4,3)D NOESY-HCCH spectrum. Figure 8 shows representative strip plots from the (4,3)D ^{1}H TOCSY-HCCH spectrum acquired for Ubiquitin in measurement time of $\sim$15 h (S/N: 10 $\pm$ 7). Nearly all the expected ^{1}H–^{1}H correlations were observed in the (4,3)D GFT spectra.

(4,3)D ^{13}C-TOCSY-HCCH

The (4,3)D ^{13}C-TOCSY-HCCH was devised to provide intra-residue ^{13}C chemical shifts. In this experiment, the ^{13}C magnetization from all ^{13}C nuclei in a given amino acid is transferred to the methyl carbon within the same amino acid by isotropic mixing (Figs. 2 and 3). Figure 9 shows

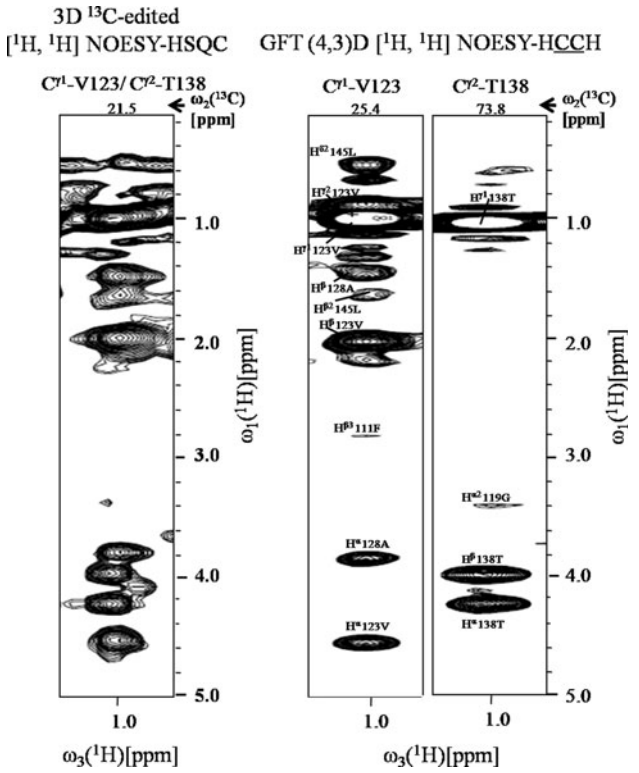

Fig. 7 $\{\omega_1\ (^1H), \omega_3\ (^1H)\}$ strips from 3D ^{13}C-edited NOESY-HSQC showing two overlapping residues ($^{13}C^{\gamma 1}$ (V123) and $^{13}C^{\gamma 2}$ (T138)) that are resolved in the (4,3)D GFT NOESY-HCCH spectrum due to differences in their $^{13}C^{neigh}$ chemical shifts ($^{13}\overline{C^{\beta}}$ (V123) ~35 ppm; $^{13}C^{\beta}$ (T138) ~70 ppm), thereby facilitating unambiguous assignment of the NOEs. Note that the Threonine peaks are aliased (Fig. 4)

representative strip plots from the (4,3)D ^{13}C-TOCSY-HCCH spectrum acquired for Ubiquitin in measurement time of ~9.5 h (S/N: 8 ± 5). Nearly all the expected ^{13}C–^{13}C correlations were observed in the (4,3)D GFT spectra.

The above experiments demonstrate the utility of modulating the chemical-shifts of $^{13}C^{met}$ with that of its directly attached ^{13}C nucleus. This imparts significant dispersion in the spectral region containing ^{13}C–^{1}H cross peaks of CH_3 groups belonging to Ala, Ile, Leu, Met, Thr and Val residues. This in turns aids in unambiguous resonance assignments of $^{13}CH_3$ groups and obtaining accurate distance constraints involving methyl groups. A few practical considerations regarding the experiments are discussed in the following. First, the maximum chemical shift evolution of $^{13}C^{met}$ (t_{max}) during t_2 is limited to 14 ms (Fig. 3) due to constant-time evolution. One can extend the chemical shift evolution periods by using semi-constant time evolution albeit at the cost of increased measurement time. However, $^{13}C^{met}$ (t_{max}) of 4–5 ms is sufficient in most cases due to good dispersion of peaks (Fig. 4). Second, while the RF

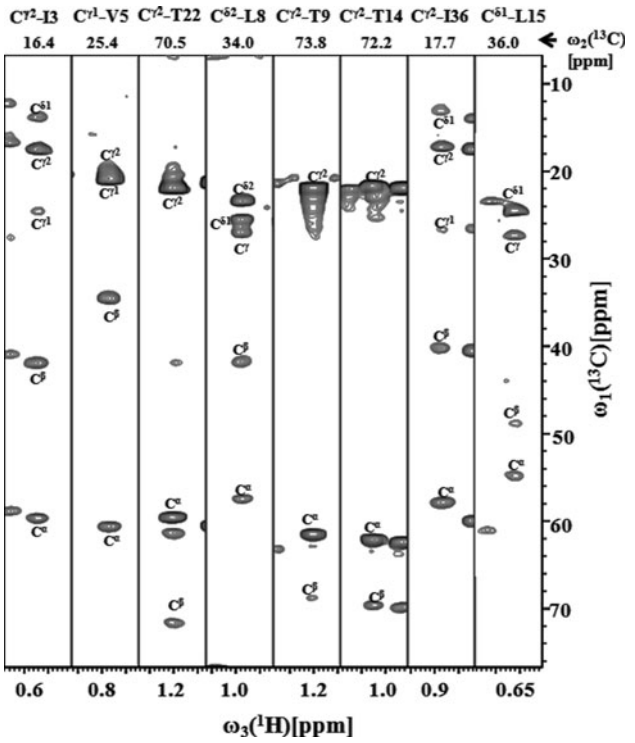

Fig. 8 Representative $\{\omega_1\ (^1H), \omega_3\ (^1H)\}$ strips from GFT (4,3)D ^1H-TOCSY-HCCH spectrum acquired for ubiquitin. Chemical shifts along ω_2 ($\Omega(^{13}\overline{C^{met}}) - \Omega(^{13}C^{neigh})$) and the residue number is indicated on the *top* of each strip. Labels on cross peaks in each strip indicate the respective chemical shift assignments. Note that the Threonine peaks are aliased (see Fig. 4)

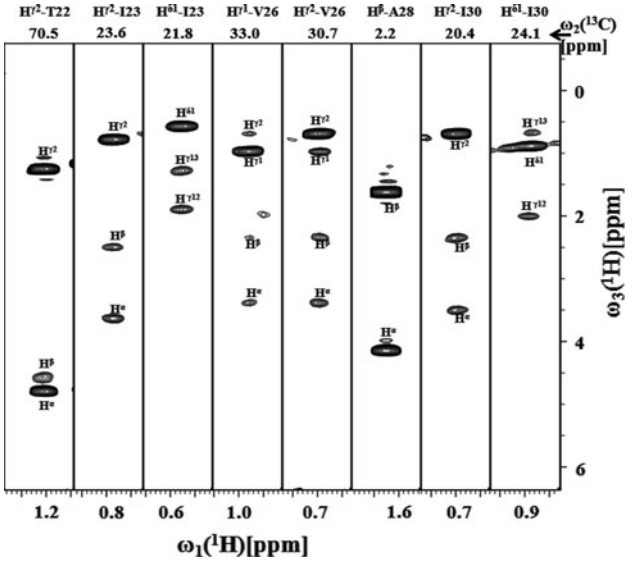

Fig. 9 Representative $\{\omega_1\ (^{13}C), \omega_3\ (^1H)\}$ strips from GFT (4,3)D ^{13}C-TOCSY-HCCH spectrum acquired for ubiquitin. Chemical shift along ω_2 ($\Omega(^{13}\overline{C^{met}}) - \Omega(^{13}C^{neigh})$) and the residue number are indicated on the *top* of each strip. Labels on cross peaks in each strip indicate the respective chemical shift assignments. Note that the Threonine peaks are aliased (see Fig. 4)

pulse scheme shown in Fig. 3 does not have an explicit scheme for suppression of the solvent (H_2O) line, a WATERGATE module (Cavanagh et al. 2007) can be incorporated during the reverse INEPT step, prior to detection. This is important for samples dissolved in 90% H_2O. Third, the choice of the carrier frequency for ^{13}C r.f. pulses and the scaling factor (κ) plays an important role. A shift in carrier frequency results in a uniform shift of the distribution (Fig. 1) whereas a change in the scaling factor impacts (1) the spectral dispersion (and thus the range of chemical shifts) and (2) the sensitivity of the experiment due to non-constant time evolution of $^{13}C^{neigh}$ (t_2) (Fig. 3). The chemical shift distribution shown in Fig. 3 was generated assuming a ^{13}C carrier frequency of 40 ppm and a scaling factor (κ) of 1.0. This results in the chemical shifts of different methyl groups in the range of −20–80 ppm for the two linear combination of chemical shifts: $\Omega(^{13}C^{met}) \pm \Omega(^{13}C^{neigh})$. However, it is not necessary to acquire both the linear combinations in the (4,3)D experiments. Either of the shift combination can selectively be chosen for detection along ω_2. The appropriate choice is based on the resolution obtained in the 2D $\{\omega_2$: $\Omega(^{13}C^{met}) \pm \kappa*\Omega(^{13}C^{neigh})$, ω_3:$^1H^{met}\}$ projection of these spectra which can be acquired rapidly with different linear combinations and scaling factors. For instance, the shift combination: $\Omega(^{13}C^{met}) - \Omega(^{13}C^{neigh})$ was found to be appropriate in the present study. The spectral width and the carrier position can then be adjusted appropriately so as to alias the peaks belonging to the methyl groups of Threonine which are well separated from the rest of the methyl group containing amino acids. Thus, with the ^{13}C carrier frequency set to 40 ppm ($\kappa = 1$), a spectral width of 60–70 ppm can be chosen which is about twice the spectral width required for a conventional 3D ^{13}C-edited NOESY-HSQC. Thus, the minimal measurement time of the GFT (4,3)D experiments is a factor of 2.0 more than the conventional congeners. Fourth, the experiments have an inbuilt filter to selectively detect ^{13}C nuclei that are attached only to one neighboring -^{13}C nucleus. This is due to the delay, $2\tau_2$, adjusted to $1/2J_{CC}$ ($\sim$14.0 ms) to transfer the magnetization from $^{13}C^{met}$ to its neighboring ^{13}C nucleus. Thus, any ^{13}C site directly attached to two or more ^{13}C nuclei results in the generation of higher order coherences, which are not detected. This is useful for suppressing peaks belonging to H^{γ}/C^{γ} of Arg and H^{δ}/C^{δ} of Lys, which overlap with those of methyl protons (Atreya and Chary 2001). The delay, $2\tau_1$, also renders a loss in sensitivity of GFT experiments compared to the conventional 3D ^{13}C-edited congeners, which employ 2D [^{13}C, ^1H] HSQC. The sensitivity loss (of the HCCH part of the GFT experiment compared to 2D HSQC) is less than 25% for non-deuterated proteins with molecular mass <20 kDa and amounts to a factor of $\sim$2 for proteins with molecular mass $\sim$40 kDa. This was estimated using the expression for signal loss in 2D HSQC described by Tugarinov et al. (2003) arising from transverse relaxation of methyl proton and carbon described therein.

Conclusions

In summary, we have developed three GFT NMR experiments, which simplify resonance assignment of methyl groups in proteins and aid in structure determination. The experiments are based on the observation that joint sampling of chemical shifts of the methyl carbon and its directly attached carbon nucleus separates the methyl group containing amino acids into distinct spectral regions. These experiments provide 4D spectral information with high sensitivity and resolution. Further spectral simplification can be achieved by combining this method with selective unlabeling of amino acids (Atreya and Chary 2001; Tugarinov and Kay 2004b). In addition, measurement times can be further reduced by combining data acquisition with other approaches for rapid data collection (Atreya and Szyperski 2005). Taken together, these experiments will have a range of applications in side-chain resonance assignment and structure determination of proteins and their complexes.

Acknowledgments The facilities provided by NMR Research Centre at IISc supported by Department of Science and Technology (DST), India is gratefully acknowledged. HSA acknowledges support from DST-SERC research award. GJ and AT acknowledge fellowship from Council of Scientific and Industrial Research (CSIR) and UGC, India. PDS acknowledges support from the Wellcome Trust International Senior Research Fellowship in Biomedical Science, WT081643MA. We thank Dr. John Cort, Pacific Northwest National Laboratory, for providing the Ubiquitin plasmid.

References

Anglister J, Grzesiek S, Wang AC, Ren H, Klee CB, Bax A (1994) H-1, C-13, N-15 nuclear-magnetic-resonance backbone assignments and secondary structure of human Calcineurin-B. Biochemistry 33:3540–3547

Atreya HS, Chary KVR (2001) Selective 'unlabeling' of amino acids in fractionally C-13 labeled proteins: an approach for stereospecific NMR assignments of CH_3 groups in Val and Leu residues. J Biomol NMR 19:267–272

Atreya HS, Szyperski T (2005) Rapid NMR data collection. Methods Enzymol 394:78–108

Barnwal RP, Atreya HS, Chary KVR (2008) Chemical shift based editing of CH3 groups in fractionally C-13-labelled proteins using GFT (3, 2)D CT-HCCH-COSY: stereospecific assignments of CH3 groups of Val and Leu residues. J Biomol NMR 42:149–154

Bartels C, Xia TH, Billeter M, Güntert P, Wüthrich K (1995) The program Xeasy for computer-supported NMR spectral-analysis of biological macromolecules. J Biomol NMR 6:1–10

Cavanagh J, Fairbrother WJ, Palmer AG, Rance M, Skelton NJ (2007) Protein NMR spectroscopy. Elsevier Academic Press, San Diego

Clore GM, Kay LE, Bax A, Gronenborn AM (1991) Four-dimensional C-13/C-13-edited nuclear overhauser enhancement spectroscopy of a protein in solution—application to Interleukin 1-Beta. Biochemistry 30:12–18

Coggins BE, Venters RA, Zhou P (2005) Filtered backprojection for the reconstruction of a high-resolution (4, 2)D CH3-NH-NOESY spectrum on a 29 kDa protein. J Am Chem Soc 127: 11562–11563

Delaglio F, Grzesiek S, Vuister GW, Zhu G, Pfeifer J, Bax A (1995) Nmrpipe—a multidimensional spectral processing system based on unix pipes. J Biomol NMR 6:277–293

Farmer BT, Mueller L (1994) Simultaneous acquisition of C-13, N-15 -separated and N-15, N-15 -separated 4D gradient-enhanced NOESY spectra in proteins. J Biomol NMR 4:673–687

Galius V, Leontiou C, Richmond T, Wider G (2008) Projected H-1, N-15 -HMQC- H-1, H-1—NOESY for large molecular systems: application to a 121 kDa protein-DNA complex. J Biomol NMR 40:175–181

Gardner KH, Konrat R, Rosen MK, Kay LE (1996) An (H)C(CO)NH-TOCSY pulse scheme for sequential assignment of protonated methyl groups in otherwise deuterated N-15, C-13-labeled proteins. J Biomol NMR 8:351–356

Gardner KH, Rosen MK, Kay LE (1997) Global folds of highly deuterated, methyl-protonated proteins by multidimensional NMR. Biochemistry 36:1389–1401

Gross JD, Gelev VM, Wagner G (2003) A sensitive and robust method for obtaining intermolecular NOEs between side chains in large protein complexes. J Biomol NMR 25:235–242

Grzesiek S, Wingfield P, Stahl S, Kaufman JD, Bax A (1995) Four-dimensional N-15-separated NOESY of slowly tumbling perdeuterated N-15-enriched proteins—application to Hiv-1 Nef. J Am Chem Soc 117:9594–9595

Kainosho M, Torizawa T, Iwashita Y, Terauchi T, Mei Ono A, Güntert P (2006) Optimal isotope labeling for NMR protein structure determination. Nature 440:52–57

Kay LE, Ikura M, Zhu G, Bax A (1991) Four-dimensional heteronuclear triple resonance NMR spectroscopy of isotopically enriched proteins for sequential assignments of backbone atoms. J Magn Reson 91:422–428

Kay LE, Xu GY, Singer AU, Muhandiram DR, Forman-kay JD (1993) A gradient-enhanced HCCH TOCSY experiment for recording side-chain H-1 and C-13 correlations in H2O samples of proteins. J Magn Reson Ser B 101:333–337

Kim S, Szyperski T (2003) GFT NMR, a new approach to rapidly obtain precise high-dimensional NMR spectral information. J Am Chem Soc 125:1385–1393

Kock M, Griesinger C (1994) Fast NOESY experiments—an approach for fast structure determination. Angew Chem Intl Ed 33:332–334

Lee W, Revington MJ, Arrowsmith C, Kay LE (1994) A pulsed-field gradient isotope-filtered 3D C-13 HMQC-NOESY experiment for extracting intermolecular NOE contacts in molecular-complexes. FEBS Lett 350:87–90

Logan TM, Olejniczak ET, Xu RX, Fesik SW (1992) Side-chain and backbone assignments in isotopically labeled proteins from 2 heteronuclear triple resonance experiments. FEBS Lett 314:413–418

Muhandiram DR, Farrow NA, Xu GY, Smallcombe SH, Kay LE (1993a) A gradient C-13 NOESY-HSQC experiment for recording NOESY spectra of C-13-labeled proteins dissolved in H2O. J Magn Reson Ser B 102:317–321

Muhandiram DR, Xu GY, Kay LE (1993b) An enhanced-sensitivity pure absorption gradient 4D N-15, C-13-edited NOESY experiment. J Biomol NMR 3:463–470

Qiu XB, Shao YM, Miao S, Wang L (2006) The diversity of the DnaJ/Hsp40 family, the crucial partners for Hsp70 chaperones. Cell Mol Life Sci 63:2560–2570

Rosen MK, Gardner KH, Willis RC, Parris WE, Pawson T, Kay LE (1996) Selective methyl group protonation of perdeuterated proteins. J Mol Biol 263:627–636

Shen Y, Atreya HS, Liu G, Szyperski T (2005) G-matrix fourier transform NOESY-based protocol for high-quality protein structure determination. J Am Chem Soc 127:9085–9099

Snyder DA, Xu YQ, Yang DW, Bruschweiler R (2007a) Resolution-enhanced 4D N-15/C-13 NOESY protein NMR spectroscopy by application of the covariance transform. J Am Chem Soc 129:14126–14127

Snyder DA, Zhang F, Brueschweiler R (2007b) Covariance NMR in higher dimensions: application to 4D NOESY spectroscopy of proteins. J Biomol NMR 39:165–175

Swain S, Atreya HS (2008) A method to selectively detect a desired linear combination of chemical shifts in GFT projection NMR spectroscopy. Open Magn Reson J 1:95–103

Szyperski T, Atreya HS (2006) Principles and applications of GFT projection NMR spectroscopy. Magn Reson Chem 44:S51–S60

Tugarinov V, Kay LE (2004a) An isotope labeling strategy for methyl TROSY spectroscopy. J Biomol NMR 28:165–172

Tugarinov V, Kay LE (2004b) Stereospecific NMR assignments of prochiral methyls, rotameric states and dynamics of valine residues in malate synthase G. J Am Chem Soc 126:9827–9836

Tugarinov V, Kay LE (2005) Methyl groups as probes of structure and dynamics in NMR studies of high-molecular weight proteins. ChemBioChem 6:1567–1577

Tugarinov V, Hwang PM, Ollerenshaw JE, Kay LE (2003) Cross-correlated relaxation enhanced H-1-C-13 NMR spectroscopy of methyl groups in very high molecular weight proteins and protein complexes. J Am Chem Soc 125:10420–10428

Tugarinov V, Hwang PM, Kay LE (2004) Nuclear magnetic resonance spectroscopy of high-molecular-weight proteins. Ann Rev Biochem 73:107–146

Tugarinov V, Choy WY, Orekhov VY, Kay LE (2005a) Solution NMR-derived global fold of a monomeric 82-kDa enzyme. Proc Natl Acad Sci USA 102:622–627

Tugarinov V, Kay LE, Ibraghimov I, Orekhov VY (2005b) High-resolution four-dimensional H-1-C-13 NOE spectroscopy using methyl-TROSY, sparse data acquisition, and multidimensional decomposition. J Am Chem Soc 127:2767–2775

Vuister GW, Clore GM, Gronenborn AM, Powers R, Garrett DS et al (1993) Increased resolution and improved spectral quality in four-dimensional C-13/C-13-separated HMQC-NOESY-HMQC spectra using pulsed-field gradients. J Magn Reson Ser B 101:210–213

Wüthrich K (1986) NMR of proteins and nucleic acids. Wiley, New York, pp 1–292

Xia YL, Yee A, Arrowsmith CH, Gao XL (2003) H-1(C) and H-1(N) total NOE correlations in a single 3D NMR experiment. N-15 and C-13 time-sharing in t(1) and t(2) dimensions for simultaneous data acquisition. J Biomol NMR 27:193–203

Xia YL, Veeraraghavan S, Zhu Q, Gao XL (2008) Fast (4, 3)D GFT-TS NMR for NOESY of small to medium-sized proteins. J Magn Reson 190:142–148

Zheng DY, Huang YPJ, Moseley HNB, Xiao R, Aramini J et al (2003) Automated protein fold determination using a minimal NMR constraint strategy. Protein Sci 12:1232–1246

Zwahlen C, Gardner KH, Sarma SP, Horita DA, Byrd RA, Kay LE (1998) An NMR experiment for measuring methyl-methyl NOEs in C-13-labeled proteins with high resolution. J Am Chem Soc 120:7617–7625